Pergamon

Cement and Concrete Research 31 (2001) 1785–1791

CEMENT AND CONCRETE RESEARCH

Internal stress within hardened cement paste induced through thermal mismatch
Calcium hydroxide versus calcium silicate hydrate

Erland M. Schulson[a,]*, Ian P. Swainson[b], Thomas M. Holden[b]

[a]*Thayer School of Engineering, Dartmouth College, 8000 Cummings Hall, Hanover, NH 03755-8000, USA*
[b]*National Research Council of Canada, Chalk River, Ontario, Canada K0J IJ0*

Received 3 January 2001; accepted 18 May 2001

Abstract

Neutron diffraction experiments have established that internal strain develops within the calcium hydroxide (CH) phase of hardened Portland cement paste when the material is cooled. The effect is attributed to thermal mismatch between CH and calcium silicate hydrate (C-S-H). It leads to internal stresses that are estimated to reach maximum values at 80 K of around 30 ± 20 MPa along the crystallographic *c* direction and around −40 ± 20 MPa along the *a* direction. © 2001 Elsevier Science Ltd. All rights reserved.

Keywords: Neutron diffraction; Thermal expansion; Calcium hydroxide

1. Introduction

When hardened Portland cement paste is cooled to below the bulk freezing point of water, internal stress develops. If sufficiently large, the stress initiates cracks. Degradation ensues and premature failure follows. How the stress originates is the issue.

One source is the formation of ice from pore water. When freezing begins within nearly saturated material, water begins to migrate through a system of interconnected pores, either towards freezing sites or away from them. In the first case, the migration is driven by a gradient in chemical potential, and pressure is generated through the growth of crystals [1,2], in the manner of ice lenses. In the second case, it is driven by the volume expansion that accompanies the transformation, and pressure develops in a hydraulic manner [3]. In both cases, the internal pressure induces tensile stress which, if large enough, can crack the calcium silicate hydrate (C-S-H) matrix. This process is termed freeze/thaw damage and is well recognized (see Ref. [4] for a review).

Another source of internal stress, and the one to which this paper relates, is the thermal mismatch between calcium hydroxide (CH), or portlandite, and C-S-H. CH typically constitutes 20% to 25% of the volume of the solid products of hydration and is present within the microstructure either in the form of thin platelets whose "diameter" can reach tens of micrometers, or, during later stages of hydration, as more massive deposits. CH is a member of the hexagonal crystal family (space group P3m1) and is both thermally and elastically anisotropic. Along the crystallographic *a* direction, both the linear coefficient of thermal expansion and the elastic compliance are smaller than those of C-S-H, while along the *c* direction both properties are larger than those of the matrix. The thermal anisotropy, which is of interest here, implies that upon cooling from the temperature of hydration, CH become compressed in the *a* direction and extended in the *c* direction provided that cohesion is maintained with the matrix. Upon heating, the reverse is expected. As a result, internal stresses are expected to develop within CH and, correspondingly, within the C-S-H matrix.

To explore this hypothesis and to assess the magnitude of the internal stresses so induced, neutron diffraction experiments were performed on hardened Portland cement

---

* Corresponding author. Tel.: +1-603-646-2888; fax: +1-603-646-3856.
E-mail address: erland.schulson@dartmouth.edu (E.M. Schulson).

PII: S0008-8846(01)00554-3

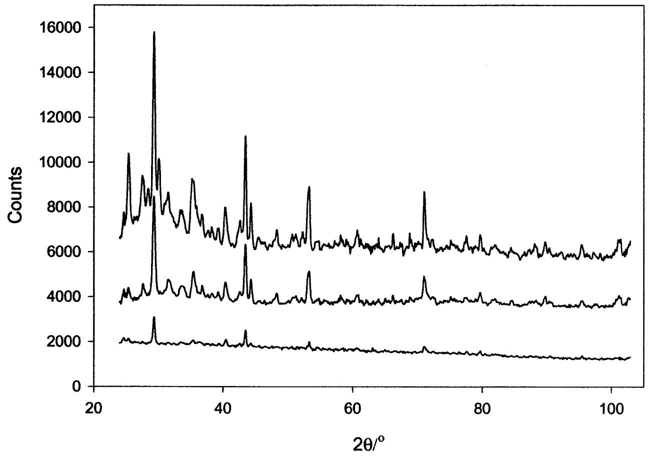

Fig. 1. Neutron diffraction patterns from CD: from powder prepared by grinding solid rod under heavy water (top), from solid rod (middle), and from powder prepared by grinding solid rod in moist air (bottom). The data were rescaled and the different curves displaced vertically so that they all fit the same plot.

paste, which was cooled to temperatures of 20 K. This paper offers a first report on the work.

2. Experimental procedure

Specimens of hardened Portland cement paste of water/cement ratio 0.36 were prepared and then examined in the manner described in an earlier paper [5]. Type II Portland cement was mixed with *heavy* water, cast into cylindrical moulds (5 mm diameter, 50 mm length), removed after 3 days, and then allowed to hydrate (i.e., deuterate) for about 3 months under lime-saturated heavy water at room temperature. Subsequently, they were sealed in vanadium tubes and purged in helium at atmospheric pressure. The neutron diffraction experiments were performed with neutrons of 0.13286-nm wavelength using the C2 spectrometer located at the NRU reactor at Chalk River Laboratories. Strains within the CD[1] phase were measured from displacements in the diffraction angles for various Bragg planes. To obtain the highest resolution, the higher angle diffraction peaks were employed.

Two series of experiments were performed. In the first, the temperature of the specimen was lowered from 280 to 20 K in increments of 20 K. In the second series, it was lowered from room temperature to 227 K in increments of 5 K. The first series was designed to examine the character of thermal contraction to temperatures approaching 0 K; the second, to determine whether the formation of ice, reported elsewhere [5,6], affected the measurements. Before each run the wait-time to allow thermal equilibrium was ~20 min; the scan-time was ~2 h. The temperature was accurate to ±0.3 K.

Two $Ca(OD)_2$ reference samples that were assumed to be stress-free were employed. One was prepared from CaO (99.0% purity) and heavy water (99.85 wt.% D_2O) in the form of free powder. The other was made by grinding a piece of the hardened cement paste *under heavy water*. Grinding in moist air is to be avoided for, upon exposing untransformed clinker, that procedure leads to additional hydration and to the incorporation into the transformation product of hydrogen whose cross-section for the incoherent scattering of thermal neutrons is much larger than that of deuterium, resulting in greatly reduced diffraction intensities. Fig. 1 illustrates this point. That hydration was not complete after about 3 months under water is consistent with the diffusion-limited character of the process during its later stage, as evident from studies employing quasi-elastic neutron scattering [7].

3. Results and analysis

Fig. 2a and b shows as a function of temperature the *a* and *c* lattice parameters of CD, both as a constrained component of the hardened paste and as free powder prepared from CaO and D_2O. The lattice parameters were obtained from the diffraction patterns using the standard Rietveld-based analysis [8]. Several points are noteworthy.

3.1. Lattice parameters

The lattice parameters at 280 K, the highest temperature shown, are comparable to the values $a=0.3593$ nm and $c=0.4909$ nm for CH, reported earlier [9].

3.2. Setting strains

Both lattice parameters are larger in the constrained state than in the free state at the start of cooling, i.e., after hardening. At 280 K, for instance, *a* is greater by 0.064% and *c*, by 0.12%. These differences are greater than measurement error and are thus considered to be significant. One explanation is that the differences reflect a slightly larger unit cell, owing perhaps to a higher concentration of impurities — i.e., point defects — within the product that formed within the C-S-D matrix. Another is that the constrained material may contain a relatively high concentration of stacking faults. Planar defects of this kind would not be surprising, for CD is isostructural with CdI_2 and this material exhibits a high propensity for faulting [10]. Moreover, stacking faults have already been reported in $Ca(OH)_2$, albeit upon heating [11]. The other explanation is that residual tensile strains and stresses may have developed within the C-S-D matrix during hardening that were then transmitted to CD, reminiscent of distortions that

---

[1] In this discussion, the portlandite and the matrix that formed through reactions between cement and heavy water are denoted CD and C-S-D, respectively.

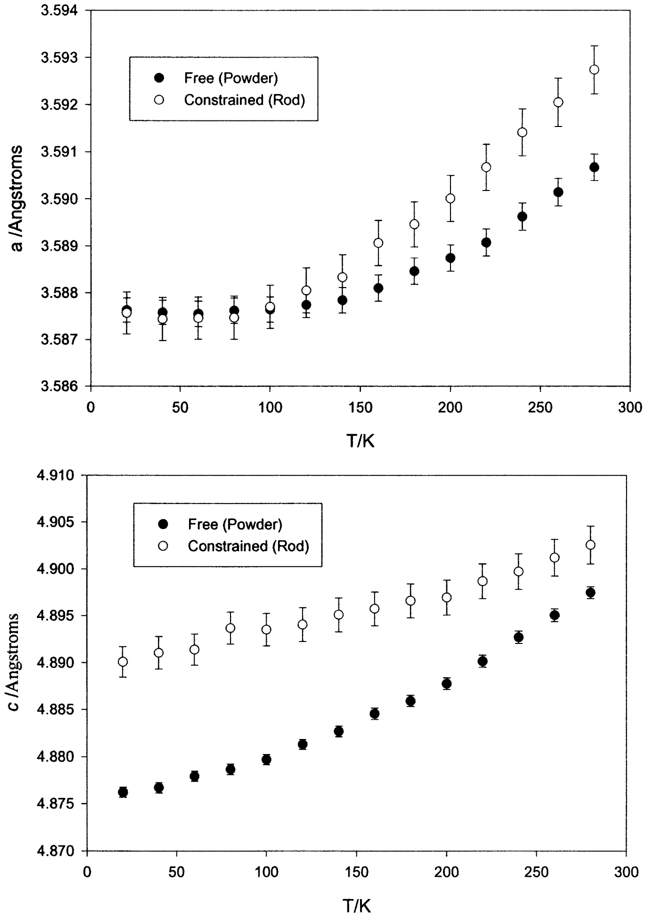

Fig. 2. Lattice parameters *a* and *c* of CD as a constituent in hardened cement paste constrained within a cylindrical rod and as free powder vs. temperature.

were detected by Laue asterism in X-ray diffraction spots from $Ca(OH)_2$ crystals that were formed during hydration of cement [12]. To assess the third possibility, a small piece of the hardened paste was ground (under heavy water), dried, and then examined in the manner described above. The results were mixed. Grinding reduced the *a* parameter by only 0.02%, which is similar to the error of measurement, but decreased the *c* parameter by 0.07%, which is outside the error. It is perhaps significant that CD is elastically stiffer than C-S-D along the *a* direction, but more compliant along the *c* direction (see Appendix A), and so could have been strained less in the *a* direction than in the *c* direction in the first place. Of course, there is the issue here — as is commonly the case when measuring residual strains using diffraction techniques — of whether the powder was ground finely enough to allow stresses to completely relax — in this case, finer than the CD crystals, whose size was probably distributed — but not so fine as to have introduced an unduly large concentration of additional deformation damage in the form of dislocations, stacking faults, and possibly twins. These points we cannot assess, for we measured neither the particle size distribution nor the sizes and shapes of CD; nor did we examine the microstructure of the ground powder. Our view, therefore, without making too much of the point until a more systematic study can be performed, is that "setting strains" cannot be ruled out as a contributing factor to the difference in lattice parameters between the confined and free states of CD.

3.3. Thermal expansion coefficients of CD

The *a* and *c* parameters, in both the confined and free states of CD, decrease with decreasing temperature, as is normal. Also, the linear thermal expansion coefficients along the *a* and the *c* crystallographic directions, respectively, $\alpha_a=(1/a)(da/dT)$ and $\alpha_c=(1/c)(dc/dT)$, become smaller as temperature (T) decreases, as is evident from the decreasing slope, da/dT, of the curves. This, too, is normal behavior. The coefficients, in fact, appear to tend to zero as temperature tends to zero, in keeping with thermodynamics. At higher temperatures ($T \gtrsim 180$ K) the coefficients are approximately independent of temperature and, for the free state, have average values (obtained from the two series of experiments) of $\alpha_a=(7.5\pm0.5)\times10^{-6}$/K and $\alpha_c=(26\pm2)\times10^{-6}$/K, in fair agreement with handbook values of $\alpha_a=9.8\times10^{-6}$/K and $\alpha_c=33\times10^{-6}$/K for the protonated version of the compound.

3.4. Internal thermal strains

The difference in lattice parameter, Δa and Δc, between the constrained and free states of CD increases with decreasing temperature. The difference is positive in one case (*c* direction) and negative in the other (*a* direction), implying the development of tensile and compressive strains, respectively. Fig. 3 shows the measured strains, obtained from the data in Fig. 2 and from the relationships

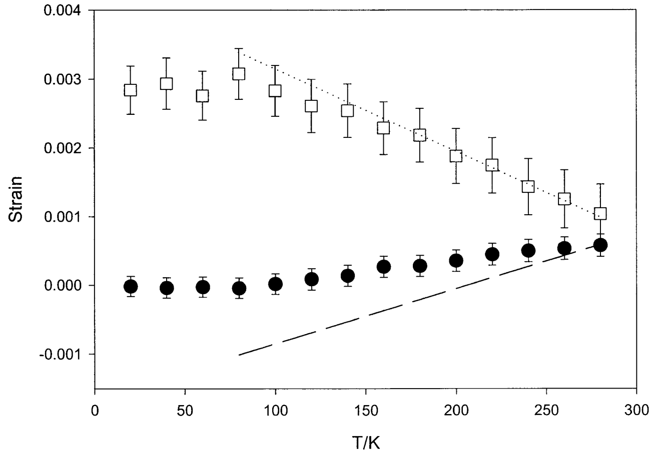

Fig. 3. Normal strains within CD measured along the *a* direction (ε_{11} closed points) and *c* direction (ε_{33} open points) vs. temperature, as well as strains computed from thermal mismatch ($\Delta\alpha$) alone (dotted and broken lines).

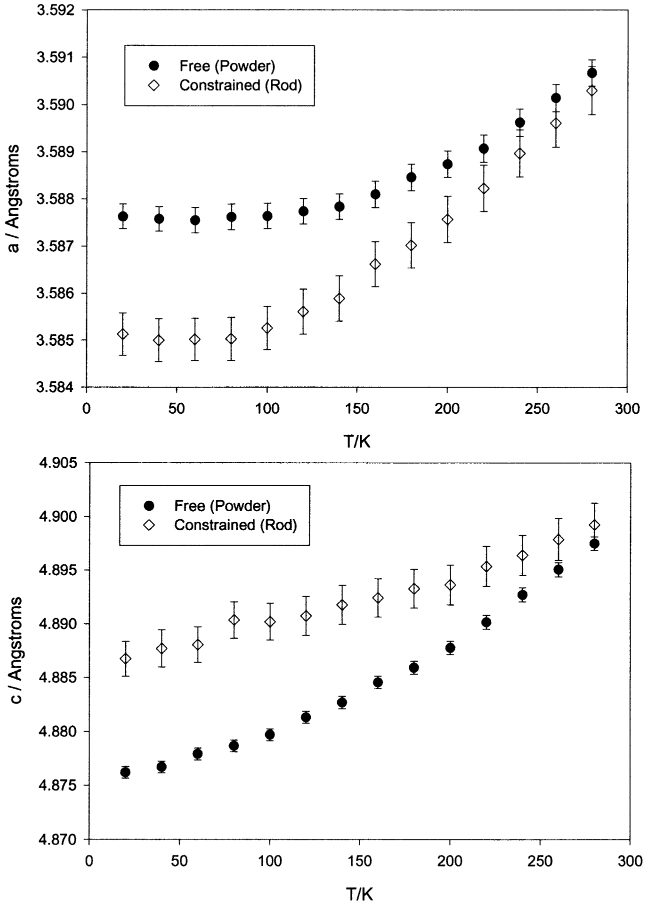

Fig. 4. Lattice parameters *a* and *c* of CD vs. temperature, corrected for "setting strains" at room temperature.

$\varepsilon_a=\varepsilon_{11}=\Delta a/a$ and $\varepsilon_c=\varepsilon_{22}=\Delta c/c$ where $\Delta a=a_{\text{const.}}-a_{\text{free}}$ and $\Delta c=c_{\text{const.}}-c_{\text{free}}$. Fig. 3 also shows thermal mismatch strains $\varepsilon_a=\Delta\alpha(a)\Delta T$ and $\varepsilon_c=\Delta\alpha(c)\Delta T$, that were computed solely from the difference in temperature ($\Delta T=$actual temperature − room temperature) and from the difference in (room temperature) values of the thermal expansion coefficients $\Delta\alpha=\alpha_{\text{C-S-D}}-\alpha_{\text{CD}}$ of the two phases along both the *a*- and *c* directions, using $\alpha_{\text{C-S-D}}=18\times10^{-6}$/K, which was taken from the value for hardened Portland cement paste [13]. Thermal mismatch accounts well for the measured strains along the *c* direction, at least to temperatures as low as ~ 180 K, above which the thermal expansion coefficient is probably not very sensitive to temperature. Along the *a* direction, thermal mismatch overestimates the strain. This difference can be understood in terms of the elastic stiffness of CD along the two directions (Appendix A). As already noted, CD is stiffer than C-S-D along the *a* direction, but more compliant along the *c* direction (i.e., $E_a=71$ GPa and $E_c=20$ GPa vs. $E_{\text{C-S-H}}\sim30$ GPa where *E* is Young's modulus). This implies that differences in thermal strains are largely accommodated by elastic deformation of portlandite in the *c* direction, but by deformation of the matrix in the *a* direction.

3.5. Internal stress

In keeping with the hypothesis upon which this work is based, d*a*/d*T* is greater for the confined state than for the free state, while d*c*/d*T* is greater for the free state. Fig. 4 illustrates these points more clearly by removing from the data in Fig. 2 the differences in the free vs. constrained values of the lattice parameters extrapolated to room temperature. Another way to view these effects is from the *c*/*a* ratio, Fig. 5. For both states before cooling, $c/a=1.364$, but with decreasing temperature, *c*/*a* decreases less rapidly in the constrained state. In other words, the constraint to thermal contraction imposed on C-S-D by CD induces within portlandite a compressive strain in the *a* direction while the constraint to contraction imposed on CD by C-S-D induces a tensile strain in the *c* direction. This implies that cooling induces internal stress. Heating would be expected to induce strains and stresses of the opposite sign.

3.6. Tensile and compressive thermal stresses

The internal thermal stress induced within CD may be calculated from the relationship:

$$\sigma_i = C_{ij}\varepsilon_j \qquad (i,j,=1,2\ldots6)$$

where σ_i are the components of the stress tensor in matrix notation and C_{ij} are the components of the elastic stiffness matrix, which is given in Appendix A. (The temperature at which the stiffness values were measured was not specified in the original paper [14] and so it is assumed that the measurements were made at room temperature. This means that the stresses computed are lower limits.) ε_j is the elastic strain in matrix notation: the component values we use are not the ones computed from thermal mismatch, for they

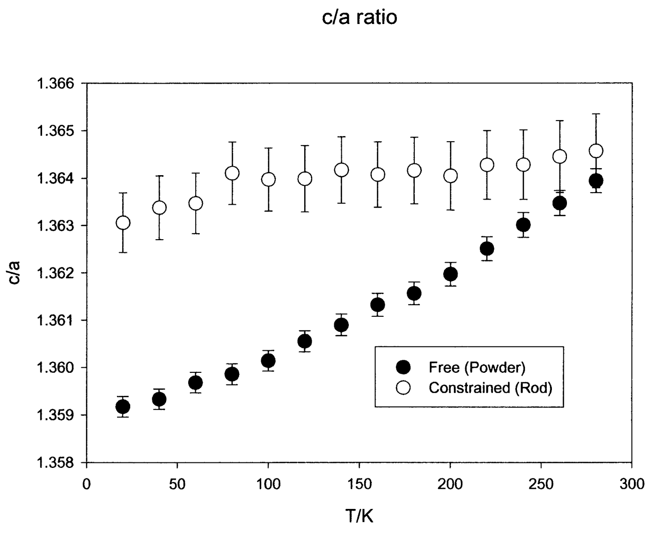

Fig. 5. Ratio of *c*/*a* from CD in constrained and free states vs. temperature.

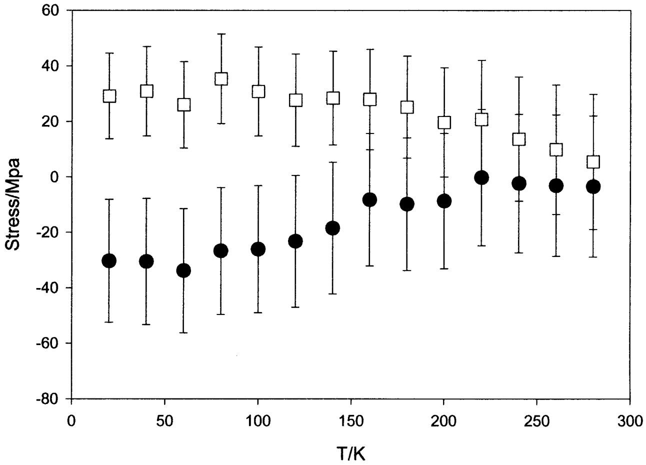

Fig. 6. Normal stresses within CD owing to thermal mismatch with C-S-D vs. temperature. $\sigma_1 = a$ direction (closed points), $\sigma_3 = c$ direction (open points).

overestimate the *a* strain, $\varepsilon_a = \varepsilon_1$, but are the ones we obtained at each temperature from the measured differences in the lattice parameters between the free and constrained states of CD, Fig. 4, after subtracting a "setting strain" of 0.00067 (see Fig. 3) to correct for zero thermal strain before cooling. Shear strains could not be determined from diffraction patterns using the standard Rietveld-based approach to fitting that we followed here, and so the measured strains are assumed to be principal strains. The stresses are thus assumed to be principal stresses. Fig. 6 shows the results. A relatively large uncertainty propagated through the calculation owing mainly to the uncertainty in strain, but also to the error in the elastic stiffness constants. Nevertheless, the analysis shows that upon decreasing temperature increasingly large compressive stresses, σ_1, developed within CD along the *a* direction (and by implication the *b* direction), while tensile stresses, σ_3, developed along the *c* direction. The stresses reached levels as high as about -40 ± 20 and 30 ± 20 MPa at ~80 K. Under conditions more characteristic of an environmental extreme in cold regions of the earth, say ~220 K, the stresses are expected to be smaller and to reach a magnitude of ~10 MPa. Note that the tensile stress appears to reach a maximum at ~80 K, a limit that could result either from cleavage across (001) planes, which are joined together by weak hydrogen bonds [9] or from decohesion along the CD/C-S-D interface. Microstructural observations of cooled material were not performed, but would be informative on this point.

4. Discussion

In considering these results, one caveat should be noted. In computing at each temperature the differences in lattice parameters between the "free" and "constrained" states of CD, and from those differences the thermal strains and stresses, we used for the free state values that were obtained from a standard whose chemical composition may have been slightly different from the composition of CD within hardened cement paste, as already noted. As a result, we may have introduced an error in the stresses. For instance, should the actual thermal expansion coefficient of free CD of paste composition be greater along the *a* direction than is that of the free standard we used, then the induced compressive stress given above would be too high. Similarly, the induced tensile stress would be too high should the actual thermal expansion coefficient along the *c* direction be lower than that of the standard. Should the actual coefficients along the *a* and *c* directions of free material be less than and greater than those of the standard, then the respective compressive and tensile stresses would be too low. Our sense, however, is that such errors would probably not be large ones and would be smaller than the error arising from uncertainties in the measurement of lattice parameters themselves and in the elastic stiffness constants. At root here is the asymmetry of the inner potential function that describes the atomic bonding. Thermal expansion is generally considered to be a "structure insensitive materials property" — i.e., insensitive to defect structure and content — and so small differences in point defect concentration are expected to have little effect on the thermal expansion coefficient. Nevertheless, it would be useful to perform the calculation again once lattice parameters have been obtained at each temperature from free CD of composition and defect structure identical to that of constrained CD.

In this same spirit, it should also be noted that we used for the elastic constants values that were obtained from CH and not from CD. This, too, could have introduced an error in the computed stresses. Again, however, any error from this source would probably be smaller than the errors in the C_{ij}'s which are between ±1.5% and ±6.1% (see Appendix A).

Perhaps the most significant point to emerge from this work is that thermal mismatch between CH and C-S-H can generate significant internal stress upon cooling. Portlandite thus has the potential to exacerbate internal damage that can accumulate within hardened cement paste upon thermal cycling, in the manner of thermal fatigue. It would seem desirable, therefore, to reduce its volume fraction, but not to zero: some is needed to maintain the pH of the pore water. The addition of the appropriate amount of silica fume or other pozzalans that activate the reaction $CH + S \rightarrow C\text{-}S\text{-}H$ should then both strengthen the hardened paste and increase its durability.

Concerning the magnitude of stresses transmitted to the matrix, the problem is essentially one of an Eshelby kind in which not only the interaction between CH and C-S-H is important, but so too are particle–particle interactions. Particle shape, which has not been a factor so far in the discussion now enters the picture. For instance, platelets of CH, when stacked, lead to the greatest local tensile stress, which acts in the region between the flat faces; coplanar platelets lead to the greatest compressive stress; and perpendicular platelets lead to the lowest value of the localized stress. More massive deposits are expected to lead to lower extreme values. This problem is currently under consideration.

Finally, it should be noted that the formation of ice within the pores of the hardened body is not expected to affect the conclusions to be drawn from this study. That ice forms under the conditions of these experiments is not a question, for this point was established through an earlier neutron diffraction study of the same material [5]. It is considered again in these proceedings [6] in light of further results. The issue here is whether the attendant crystal pressure [1,2] and/or hydraulic pressure [3] was great enough to have affected the position of the Bragg diffraction peaks from CD. To do so would have required the ability to resolve elastic strain at the level of approximately $\sigma_t/E_{\text{C-S-H}}$ where σ_t is the tensile strength of the C-S-H matrix. Assuming that $\sigma_t \sim 6$ MPa, a resolution of better than about 2×10^{-4} would have been needed. The actual resolution of the present experiments was between 1.45×10^{-4} and 1.62×10^{-4} for the *a* parameter and between 3.50×10^{-4} and 4.30×10^{-4} for the *c* parameter. Thus, changes in lattice parameter of CD caused by stresses induced within the C-S-D matrix through the freezing of pore water would not have been easily detectable within the precision employed. The idea [15] of using CD or some other crystalline phase as an internal, strain gauge, however, would appear to have merit and is one we are currently pursuing.

5. Conclusions

1. Differential thermal contraction between CH and C-S-H induces internal stress within hardened cement paste upon cooling.
2. Owing to the thermal anisotropy of CH, compressive stress develops within this phase in the crystallographic *a* (and *b*) direction and tensile stress develops in the *c* direction.
3. The stresses increase with decreasing temperature, reaching values of about -40 ± 20 MPa along the *a* direction and about 30 ± 20 MPa along the *c* direction at 80 K.

Acknowledgments

This work was sponsored by the US Federal Highway Administration through USA-CRREL, Contract No. DACA 89-97-K-0007. Discussions with Charles Korhonen of CRREL and Dr. Richard Livingston of FHWA are gratefully acknowledged.

Appendix A. Calculation of the Young's modulus of CH

With respect to the X_i ($i=1,2,3$), Cartesian coordinate systems where X_1 and X_3 are parallel to the crystallographic directions *a* and *c*, respectively, Young's moduli E_a and E_c can be calculated from the relationships $E_a = E_{11} = 1/S_{11}$ and $E_c = E_{33} = 1/S_{33}$ where S_{11} and S_{33} are components in the elastic compliance matrix S_{ij}. In turn, S_{ij} can be obtained by inverting the elastic stiffness matrix C_{ij}. Accordingly, for the -3m crystal class of which CH is a member:

$$S_{11} = (-(C_{44}C_{11}C_{33} - C_{44}C_{13}^2 - C_{33}C_{14}^2))/(-C_{44}C_{33}C_{11}^2 + 2C_{44}C_{13}^2C_{11} - 2C_{44}C_{13}^2C_{12} + C_{44}C_{12}^2C_{33} + 2C_{12}C_{33}C_{14}^2 - 4C_{13}^2C_{14}^2 + 2C_{33}C_{14}^2C_{11})$$

$$S_{33} = \frac{C_{11} + C_{12}}{(C_{33}C_{12} - 2C_{13}^2 + C_{11}C_{33})}$$

From Holuj et al. [14], C_{ij} for CH (presumably at room temperature) is given by:

$$C_{11} = 9.93 \pm 0.15 \times 10^{10}\ \text{N/m}^2$$

$$C_{33} = 3.26 \pm 0.2 \times 10^{10}\ \text{N/m}^2$$

$$C_{44} = 0.985 \pm 0.2 \times 10^{10}\ \text{N/m}^2$$

$$C_{12} = 3.62 \pm 0.2 \times 10^{10}\ \text{N/m}^2$$

$$C_{13} = 2.96 \pm 0.15 \times 10^{10}\ \text{N/m}^2$$

$$C_{14} \simeq 0.$$

Thus, $S_{11} = 0.141 \times 10^{-10}$ m^2/N and $S_{33} = 0.509 \times 10^{-10}$ m^2/N and so $E_{11} = E_a = 71$ GPa and $E_{33} = E_c = 20$ GPa.

References

[1] D. Everett, The thermodynamics of frost damage to porous solids, Trans. Faraday Soc. 57 (1961) 1541–1551.

[2] G.W. Scherer, Crystallization in pores, Cem. Concr. Res. 29 (1999) 1347–1358.

[3] T.C. Powers, Basic considerations pertaining to freezing and thawing tests, American Society for Testing and Materials, vol. 55, ASTM, Philadelphia, 1955, pp. 1132–1155.

[4] J. Marchand, R. Pleau, R. Gagne, Deterioration of concrete due to freezing and thawing, J. Skalny, S. Mindess (Eds.), Mater. Sci. Concr. IV (1995) 283–354.

[5] E.M. Schulson, I.P. Swainson, T.M. Holden, C.J. Korhonen, Hexagonal ice in hardened cement, Cem. Concr. Res. 30 (2000) 191–196.

[6] I.P. Swainson, E.M. Schulson, A neutron diffraction study of ice and water within a hardened cement paste during freeze–thaw, Cem. Concr. Res. 31 (2001) 1827–1836.

[7] R.A. Livingston, D.A. Neumann, A.J. Allen, S.A. Fitzgerald, R. Berliner, Application of neutron scattering to Portland cement, Neutron News 11 (4) (2000) 18–24.

[8] R.A. Young (Ed.), The Rietveld method, Int. Union Crystallogr. Monogr. Crystallogr. 5, Oxford University Press, 1995.

[9] H.F.W. Taylor, Cement Chemistry, Academic Press, London, 1990.

[10] R.W.G. Wyckoff, Crystal Structures, second ed., vol. 1, Interscience Publishers, New York; London; Sydney, 1963.

[11] O. Chaix-Pluchery, J. Pannetier, J. Bouillot, J.C. Niepce, Structural prereactional transformations in $Ca(OH)_2$, J. Solid State Chem. 67 (1987) 225–234.

[12] J.E. Gillott, P.J. Sereda, Strain in crystals detected by X-ray, Nature 200 (1966) 34–36.

[13] P.K. Mehta, P.J.M. Monteiro, Concrete, Prentice-Hall, New York, 1993.

[14] F. Holuj, M. Drozdowski, M. Czajkowski, Brillouin spectrum of $Ca(OH)_2$, Solid State Commun. 56 (12) (1985) 1019–1021.

[15] E.M. Schulson, Ice damage to concrete, CRREL Special Report 98-6, April 1998.